Novel Unit Cell Based on the Grounded Patch for Filter Applications

Vasa Radonić, Vesna Crnojević-Bengin
Department for Power, Electronics and Telecommunications, FTN, University of Novi Sad
Novi Sad, Serbia
vasarad@uns.ns.ac.yu, bengin@un.ns.ac.yu

Branka Jokanović
IMTEL Communiations,
Belgrade, Serbia,
branka@insimtel.com

Abstract—**Metamaterial unit cells based on the square grounded patch are proposed and applied in the microstrip filter design. Influence of geometrical parameters to performances of the unit cell is analyzed. To illustrate the potentials of the proposed unit cells, wide stopband filters of the fourth order at 3GHz are designed. End-coupled resonator is also designed by using the proposed unit cell, whose length is reduced for 69% in respect to the conventional case.**

Keywords-Metamaterials, Filters, Patch resonator

I. INTRODUCTION

Values of dielectric permittivity and magnetic permeability, as well as coefficient of refraction and characteristic impedance of materials existing in nature are limited to very small region. Existence of material with unusual values of these parameters can provide better performances of circuits and components. In the last decade, development of artificial structures which exhibit unusual electromagnetic properties, received a significant attention. Such structures, called metamaterials, consist of unit cells with subwavelength dimensions. Due to subwavelength dimensions of the unit cells, quasi-static analysis can be performed and the concept of artificial effective media can be applied. According to proper choice of the type and geometrical arrangement of the unit cells, the effective parameters of metamaterials can be made arbitrarily small or large, or even negative.

The behavior of LH media was theoretically analyzed by Russian physics Victor Veselago in the late sixties, [1]. However, the first structure that exhibits negative permittivity by decreasing the plasmon frequency into the microwave range was proposed in the mid nineties, [2]. Shortly afterwards, a particle called split-ring resonator (SRR) was introduced, that provides negative permeability at microwave frequencies, [3]. Essentially, SRRs behave as LC resonant tanks and at resonance exhibits filtering properties when properly polarized.

In microstrip architecture, negative permeability is achieved when SRR is placed next to the microstrip line, [4]. Such structure is a single negative medium and exhibits stopband characteristic in the vicinity of the resonant frequency of SRR. Although having a narrow frequency range, the configurations using SSRs have driven a lot of attention, [5], [6], [7]. However, in fabrication of SRR-based circuits, a special attention has to be paid to the resolution, i.e. to the fabrication of narrow conductive lines on small spacing which form an SRR.

In this paper, novel metamaterial microstrip structures are presented, where SRR is replaced with much simpler unit cell - a grounded square patch shown in Fig. 1. Grounded patch was initially proposed by D. Sievenpiper in electromagnetic bandgap (EBG) structures, in the design of two-dimensional metamaterials, [8], but are seldom used in microstrip applications. The main feature of EBG structures is the suppression of surface wave propagation, which increases the antenna gain and reduces the unwanted back radiation. Recently, microstrip applications of grounded patch grabbed attention, [9]. In this paper, microstrip applications of grounded patch were proposed in the design of bandstop filters. Influences of different arrangements in regard to microstrip line and geometrical parameters on performances were analyzed. To illustrate the potentials of the proposed unit cells, stopband filters of the fourth order were designed using different geometrical positions of patches. End-coupled resonator was as well designed by using the proposed unit cell.

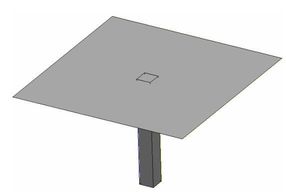

Figure 1. Unit cell - Patch resonator

II. MICROSTRIP IMPLEMENTATIONS

The grounded patch unit cell comprises of a metal square etched on the top side of the substrate, and connected by via to the ground plane on the lower side of the substrate, Fig. 1. In this paper three different positions of patch are investigated in regard to the microstrip line: patch positioned under the microstrip, next to the microstrip and embedded in the microstrip, Fig 2. In the first case, where patch is positioned under microstrip line, patch is located in the middle layer between ground and top layer (dotted line in Fig. 2a) at the minimal distance in regard to microstrip, equal to 0.1mm.

Microstrip line loaded with the grounded patch is shown in Fig. 2b. To enhance the coupling, distance between the unit cells and the microstrip line is chosen to be the minimal achievable in standard PCB technology, i.e. equal to 0.1µm. In the third case, Fig. 2c, microstrip line is extended and patch is implemented in it. Ring width around the patch and distance between patch and ring are minimal. In order to increase the inductance of unit cell via also has minimal width, equal to 100µm. The initial length of the side of the square patch was a=5mm. The circuits are realized on a 1.27mm thick Taconic CεR-10 substrate, with ε_r=9.8 and dielectric loss tangent equal to 0.0035. Conductor losses are modeled using bulk conductivity for copper. All simulations were performed using EMSight, full-wave simulator from Microwave Office. Responses of all proposed structures are compared in Fig 3.

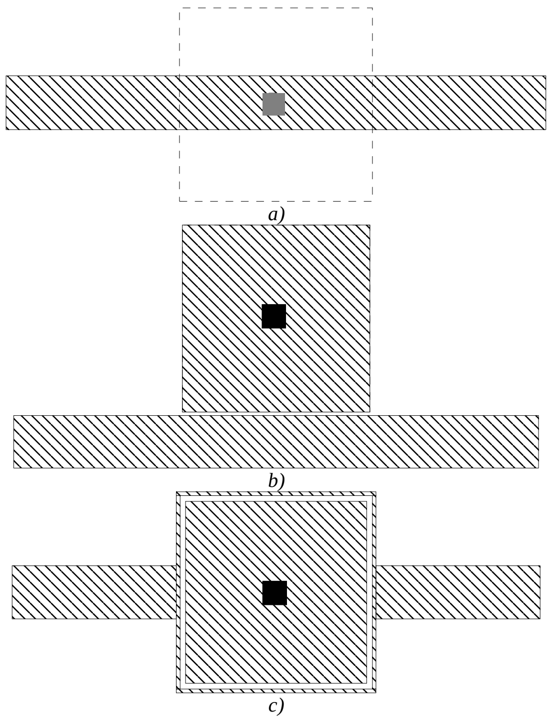

Figure 2. Proposed unit cells: a)Patch under microstrip (dotted line–bottom layer), b)Patch next to microstip, c)Patch in microstrip

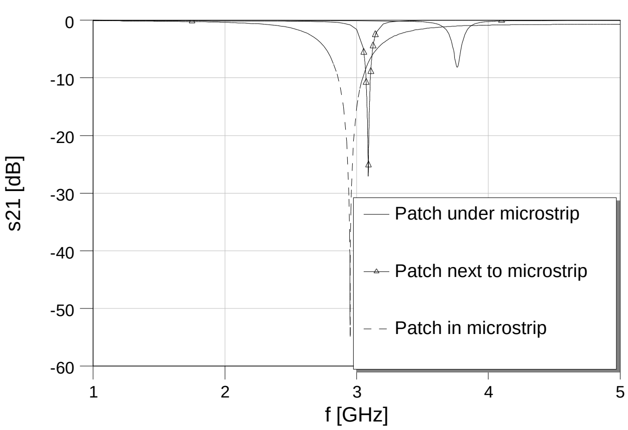

Figure 3. Responses of structures depicted in Fig. 2.

The patch structure behaves as a resonator as well as SRR, and exhibits stop characteristics when positioned near to the microstrip line. The resonant frequency of the unit cell depends on its dimensions and configurations. To investigate the influence of the patch size on the performances, outer dimensions of the patch, a, were varied. Tables I, II and III show simulation results for all structures, where f_{s1} denotes first resonant frequency, s_{21} is insertion loss at f_{s1}, B_{-3dB} and B_{-10dB} are 3dB and 10dB bandwidths, respectively.

It can be seen that patch embedded in microstrip has the lowest resonant frequency, the highest insertion losses and the widest stopband for all dimensions of the patch.

The coupling between the microstip line and the patch was analyzed by changing the distance between them in the case when patch is under the microstrip. Table IV shows simulation results for different patch height h (distance between patch and ground plane), where f_{s1} denotes first resonant frequency, s_{21} is insertion loss at f_{s1}, B_{-3dB} and B_{-10dB} are 3dB and 10dB bandwidths, respectively. It can be seen that the strong coupling between patch and transmission line makes it possible to shorten the coupling length.

In the case when the patch is positioned next to the microstrip, the distance between the patch and the microstrip is chosen to be the minimal achievable in standard PCB technology, i.e. 100µm. In this case an influence of via position was investigated. Four different marginal via positions were analyzed, Fig. 4. Simulation results are compared in Table V and in Fig.5.

TABLE I. SIMULATION RESULTS FOR PATCH UNDER MICROSTRIP LINE

***a* [mm]**	**5**	**3.1**	**2.5**	**1.5**	**0.7**
f_{s1} [GHz]	3.76	6.27	7.99	13.8	14.7
B_{-3db} [MHz]	114.1	272	364.8	679	250
B_{-10} [MHz]	na	na	na	93.6	na
s_{21} [dB]	-6.44	-9.03	-9.47	-10.8	-9.38

TABLE II. SIMULATION RESULTS FOR PATCH NEXT TO MICROSTRIP LINE

***a* [mm]**	**5**	**3.1**	**2.5**	**1.5**	**0.7**
f_{s1} [GHz]	3.09	4.68	5.59	8.24	13.5
B_{-3db} [MHz]	114	222	316	681	1200
B_{-10} [MHz]	37.5	78.8	109	236	379
s_{21} [dB]	-34.4	-42.1	-49.5	-28.6	-36.4

TABLE III. GROUNDED PATCH EMBEDDED IN THE MICROSTRIP

***a* [mm]**	**5**	**3.1**	**2.5**	**1.5**	**0.7**
f_{s1} [GHz]	2.99	4.43	5.28	7.77	13.2
B_{-3db} [MHz]	572	1190	1725	3166	5680
B_{-10} [MHz]	189.4	365	502	1000	1557
s_{21} [dB]	-52.6	-50.3	-49.8	-54	-55.6

TABLE IV. SIMULATION RESULTS FOR PATCH UNDER MICROSTRIP LINE FOR DIFFERENT PATCH HEIGHT

h_1 [mm]	**0.1**	**0.27**	**0.5**	**1**	**1.17**
f_{s1} [GHz]	3.76	3.45	3.12	2.39	1.8
B_{-3db} [MHz]	114.1	236.2	397.9	1152	1833
B_{-10} [MHz]	na	65.3	125.1	378.6	734
s_{21} [dB]	-6.44	-14.9	-21.4	-34.1	-43

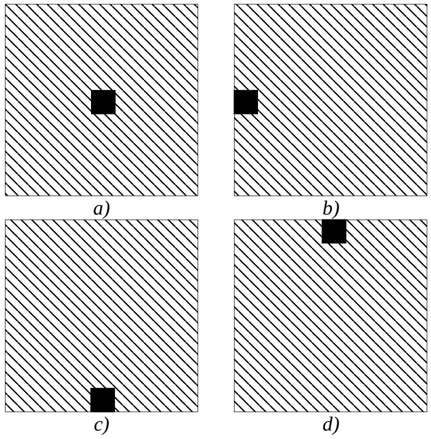

Figure 4. Via position in regard of microstrip line: a) centred, b) left, c) next to the microstrip (down), d) us far as possible from the microstrip (up)

TABLE V. INFLUENCE OF VIA POSITION TO THE PERFORMANCES

Via Position	**Centre**	**Left**	**Down**	**Up**
f **[GHz]**	3.09	2.71	2.72	2.69
f **[%]**	nd	-12.2	-12	-12.94
s_{21} **[dB]**	-27	-23.9	-23.1	-23.2
B **[MHz]**	115	85	85	79
B **[%]**	nd	-26.1	-28.7	-31.3

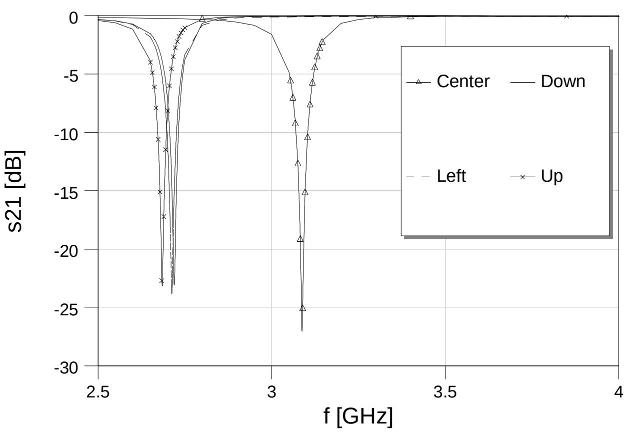

Figure 5. Influence of via postions to the performances

It can be seen that changes in the positions of via result in vast changes of the resonance. For example, maximal change in via position provides reduction for more then 24%.

Via diameter is a parameter that is very difficult to control in fabrication process. Therefore, influences of via diameter were investigated. Three different dimensions of square via are analyzed in the case where patch is embedded in microstip line: 0.1mm, 0.3mm and 0.5mm. Simulation results are depicted in Fig 6. In the Table VI, calculation results for via inductance, *L* and resonant frequency of parch, f_r are shown. Inductance of via is calculated according to its dimensions using inductance calculator.

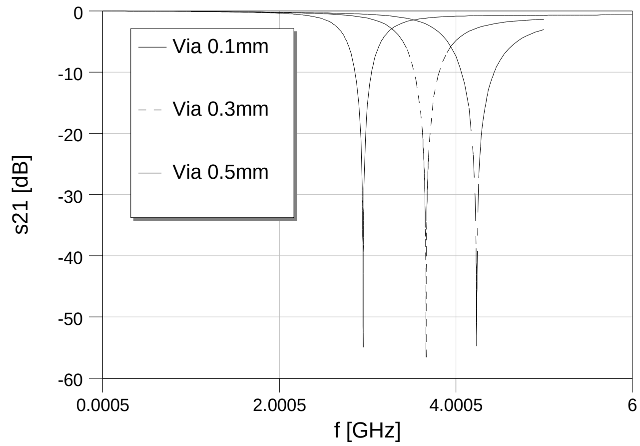

Figure 6. Influence of via dimensions to the performances in the case where patch are embeded in microstipl line

TABLE VI. INFLUENCE OF VIA DIMENSIONS TO THE PERFORMANCES

Via [mm]	**0.1x0.1**	**0.3x0.3**	**0.5x.0.5**
L **[nH]**	0.786	0.533	0.431
L **[%]**	nd	-32	-45
f_r **[GHz]**	2.95	3.66	4.24
f_r **[%]**	nd	24	43

It can be seen that small changes in the via dimensions result in high changes of the inductance, causing very large changes of the resonant frequency.

III. FILTER APPLICATIONS

To illustrate the potential of the proposed unit cell in the arbitrary choice of the filtering characteristic, stopband filters of the fourth order were designed with different geometrical arrangement of patches. Layouts of the filters are shown in Fig. 7 for outer dimensions of patches 5x5mm. Distance between patches is 0.3mm, distance between microstrip line and patch is 0.1mm and via is 0.1x0.1mm. All structures have been realized on a Taconic CεR-10 substrate. The frequency responses of the structures are shown in Fig. 8.

All proposed filters are characterized by very low insertion loss in passband and very wide bandwidth. In the filter where patches are positioned next to the line, 3dB fractional bandwidth is equal to 15.2% centered at 3.1GHz. Filter with patches positioned under microstrip line, show sharper transition for both side of stopband with suppression of more then 20dB. The filter with patches embedded in microstrip line shows 30% wide 10dB fractional bandwidth centered at 3GHz with the insertion loss of more than 30dB. Stronger coupling between patches and line is causing a small ripple at the ends of the stopband and produce dipper stopband. Using two patches symmetrically positioned with microstrip line instead of the one, produces better characteristics of some filters.

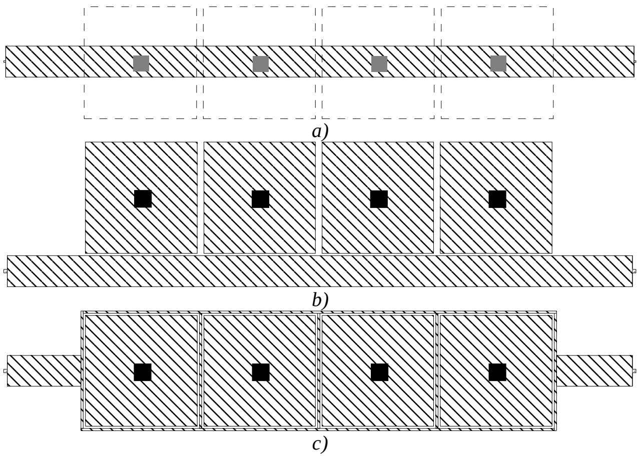

Figure 7. Proposed stopband filters: a) Patch under microstrip, b)Patch next to microstip, c) Patch in microstrip

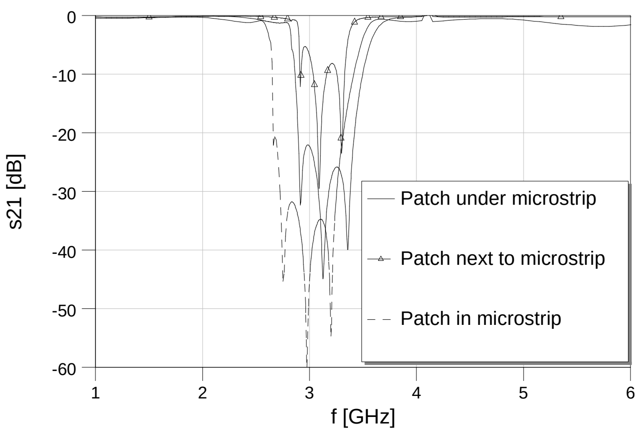

Figure 8. Simulations results for stopband filters depicted in Fig. 7

IV. End-coupled resonator

End-coupled resonator is also designed by using the proposed unit cell, where patch is embedded in resonant line, Fig. 9. This resonator is compared to a conventional $\lambda/2$ resonator with the same length and with conventional $\lambda/2$ resonator tuned to the same frequency. Simulation results are presented in Fig. 10 and in Table VI, where f_{r1} denotes resonant frequency of the first passband, B is 3-dB passband, s_{21} i s_{11} are denotes insertion losses in passband and reflection coefficient at f_{r1}, Q_L and Q_U are loaded and unloaded quality factor, respectively. Length of resonant line, l, is 5.4mm and length of tuned conventional resonator is 17.2mm.

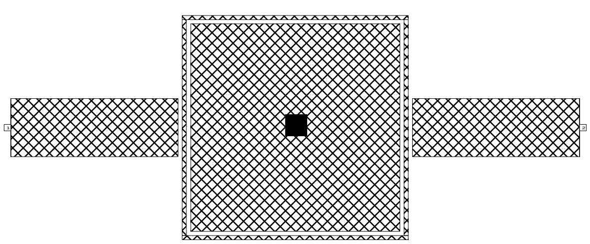

Figure 9. End-coupled resonator with patch embedded in resonant line

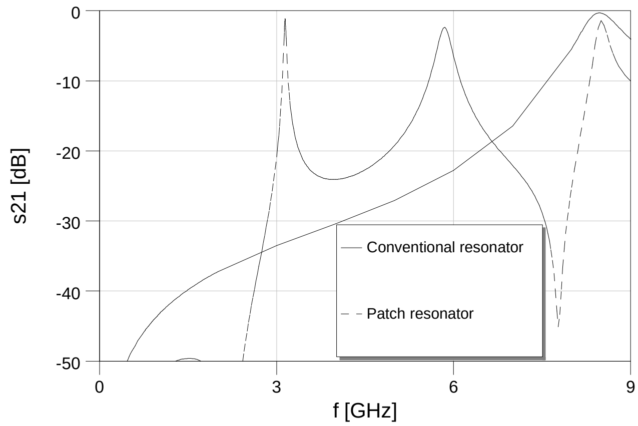

Figure 10. Comparison of simulation results for resonator with patch and conventional resonator for the same length

TABLE VII. Comparison of simulation results for resonator with patch and conventional resonator

	Convectional λ/2 resonator	Tuned conv. λ/2 resonator	Patch resonator
l [mm]	5.4	17.2	5.4
f_{r1} [GHz]	8.48	3.14	3.13
B [MHz]	761.1	38.3	49.3
s_{21} [dB]	-0.309	-1.16	-1.74
s_{11} [dB]	-27.6	-23.2	-18.9
Q_U	11.14	81.98	63.49
Q_L	162.21	349.74	192.33

In this case of patch resonator, length is reduced for 69% in respect to the conventional case. Patch resonator has wider passband, smaller length and higher insertion losses in passband in contrast to conventional resonator.

V. Conclusion

Comparative analyses of microstrip line loaded with patch unit cells have been carried out in this work. Influence of geometrical parameters on performances of the unit cell was analyzed. To demonstrate the applicability of the proposed unit cell, stopband filters of the fourth order and end-coupled resonator are designed. All filters are characterized by very low insertion loss in passband and a very wide bandwidth. Filter with patches embedded in line has 10dB fractional bandwidth equal to 30% centered at 3GHz and very sharp transition from both sides of stopband with good suppression. The proposed filter offers a very good trade-off between miniaturization and performances. The length of the proposed end-coupled resonator is reduced for 69% in respect to the conventional case.

References

[1] V. G. Veselago, “The electrodynamics of substances with simultaneously negative values of ε and μ,” *Soviet Physics Uspekhi*, vol. 10, pp.509–514, 1968,

[2] J. B. Pendry, A. J. Hoden, W. J. Stewart, and I. Youngs, “Extremely low frequency plasmons in metallic mesostructures,” *Physical Review Lett.*, vol. 76, num. 25, pp. 4773-4776, 17 June 1996,

[3] J. B. Pendry, A. J. Holden, D. J. Robbins, and W. J. Stewart, “Magnetism from conductors and enchanced nonlinear phenomena,” *IEEE Trans. on MTT*, vol. 47, no. 11, pp. 2075-2084, November 1999,

[4] V. Radonić, V. Crnojević-Bengin and B.Jokanović: „Different Approaches to the Design of Metamaterials,“ *Microwave review*, Vol.13, No.2, pp 2-7, December 2007

[5] R. Marques, J. D. Baena, M. Beruete, F. Falcone, T. Lopetegi, M. Sorolla, F. Martın and J. Garcia, “*Ab initio* analysis of frequency selective surfaces based on conventional and complementary split ring resonators”, *J. Opt. A: Pure Appl. Opt.* **7** (2005) S38–S43 January 2005.

[6] R. Marqués, J. Martel, F. Mesa, and F. Medina, “Left handed media simulation and transmission of EM waves in sub-wavelength SRR-loaded metallic waveguides”, *Phys. Rev. Lett*., vol 89, pp. 183901-03, 2002.

[7] F. Martín, F. Falcone, J. Bonache, R. Marqués, and M. Sorolla, “Miniaturized coplanar waveguide stop band filters based on multiple tuned split ring resonators”, *IEEE Microwave Wireless Comp. Lett.*, vol. 13, pp. 511-513, December 2003.

[8] D. Sievenpiper, L. Yhang, R.F.J. Broas, N. Alexopulous, E. Yablanovitch: “High-impedance electromagnetic surfaces with a forbidden frequency band,” *IEEE Tanc. Microw. Theory Tech*., Vol.47, No.11, November 1999,

[9] J. G. Lee and J. H. Lee:”Parallel Coupled Bandstop Filter Using Double Negative Coupled Transmission Line*” IEEE Microwave and optical tech. letter* Vol. 17, No. 4, April 2007